JOURNAL OF THERMOPHYSICS AND HEAT TRANSFER
Vol. 12, No. 2, April–June 1998

Investigation of High-Enthalpy Air Plasma Flow with Electrostatic Probes

Harald A. Habiger* and Monika Auweter-Kurtz†
University of Stuttgart, Stuttgart 70550, Germany

At the Institute for Space Systems of the University of Stuttgart, four plasma wind tunnels are in operation to investigate the thermochemical behavior of thermal protection systems of various space vehicles during planetary entries. To achieve a detailed understanding of the plasma conditions in a plasma wind tunnel and of the erosion mechanisms of thermal protection materials, a specific flight condition on the re-entry trajectory of a winged vehicle was investigated experimentally and numerically in detail during the last few years. Electron temperatures, electron densities, plasma potentials, electron energy functions, and particle velocities of the air plasma flow generated by a magnetoplasmadynamic plasma generator were investigated by cylindrical electrostatic single, double, and triple probes. Plasma velocities were determined with time-of-flight probes, taking advantage of natural fluctuations of the ion current densities in the air plasma flow. Using the ratio of directed and thermal ion velocities related to currents of parallel- and perpendicular-oriented probes according to the Kanal theory, the ion temperature is estimated.

Nomenclature

A = area of probe electrode
e = electron charge, $1.6021892 \times 10^{-19}$ C
$F(E)$ = electron energy distribution function
I = probe current
I_e = electron current
I_i = ion current
i_i = ion current correction factor
j_e = electron current density
j_i = ion current density
k = Boltzmann constant, 1.380662×10^{-23} J/K
l = probe length
m_e = electron mass
m_i = ion mass
n_e = electron density
n_i = ion density
r = probe radius
T_e = electron temperature
T_i = ion temperature
T_k = heavy particle temperature
U = probe voltage
V = applied external probe potential
V_F = floating potential
V_{PL} = plasma potential
v_i = directed ion velocity
v_{th} = mean thermal velocity
β = triple-probe correction factor
$\Gamma(\ )$ = gamma function
θ = angle of attack between probe and plasma flow
λ_D = Debye length, $(\varepsilon_0 kT_e/e^2 n_e)^{1/2}$
λ_{xx} = mean free path of charged particles, $xx = ei, ee, ii$
τ_l = end-effect parameter
χ_p = normalized probe potential, $e(V_{PL} - V)/kT_e$

Introduction

TO achieve a detailed understanding of the air plasma conditions in plasma wind tunnels (PWK) driven by magnetoplasmadynamic generators (MPG), and thus of the erosion mechanisms of thermal protection materials, interest is focused on the simulation and detailed investigation of a specific flight condition related to the maximum temperature at the leading edge for the re-entry of a spaceplane vehicle.[1] In addition to electrostatic probes of various types for the measurement of electron temperatures, electron densities, plasma potentials, electron energy functions, and particle velocities,[2] the properties of the air plasma flow have been experimentally investigated by optical means,[3,4] mechanical probe methods,[5] and mass spectroscopy,[6,7] as well as by numerical calculations of the plasma conditions.[8–10]

The parameters for the corresponding flight environment are a velocity of 7452 m/s at an altitude of 81.3 km, which causes a specific freestream enthalpy of 28 MJ/kg, a specific mass flow rate of 0.117 kg/(m^{2}s), and a total stagnation pressure of 400 Pa. The investigations of the corresponding arc-heated MPG air plasma flow condition with electrostatic probes were performed in the PWK2 at two cross sections, at axial distances of $x = 117$ and 467 mm to the MPG nozzle exit. At the second cross section, the required local specific freestream enthalpy of about 28 MJ/kg, and a total stagnation point pressure of about 400 Pa, are obtained.[9]

The air plasma flow is generated by the MPG plasma source RD5 (Fig. 1), having 80% nitrogen injected through the arc chamber and 20% oxygen injected in the supersonic part of the nozzle.[1] To avoid spot arc attachment on the anode, a small amount of argon is injected tangentially along the anode contour. The arc current is 1200 A, the total mass flow is 2.0 g/s air, and the ambient pressure in the PWK is about 290 Pa.

Applied Probe Theories

The applicable theory to describe the probe response is mainly determined by the influence of the probe electrode dimensions on the plasma properties.[11,12] Near the probe electrode, a thin layer called the plasma sheath, which has a thickness on the order of the Debye length, forms the boundary to

Presented as Paper 96-1864 at the AIAA 31st Thermophysics Conference, New Orleans, LA, June 17–20, 1996; received May 27, 1997; revision received Oct. 2, 1997; accepted for publication Oct. 5, 1997.

*Research Scientist, Institut für Raumfahrtsysteme, Pfaffenwaldring 31. E-mail: habiger@irs.uni-stuttgart.de. Member AIAA.

†Professor, Institut für Raumfahrtsysteme, Pfaffenwaldring 31. Member AIAA.

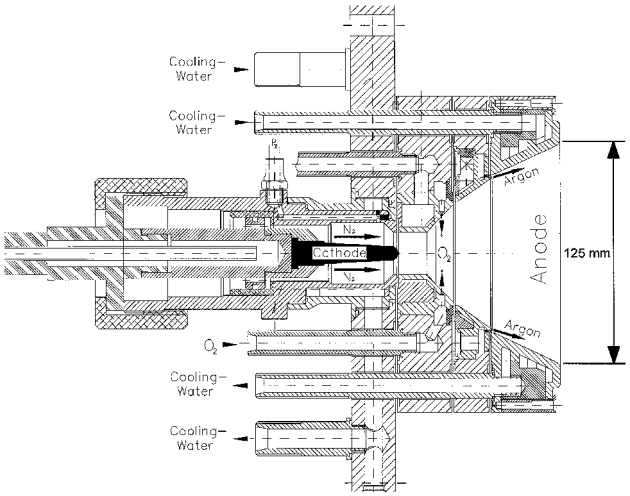

Fig. 1 Plasma generator RD5 of the PWK2-IRS.

the undisturbed plasma. Within this layer, the electron and ion number densities differ according to the applied probe potentials. The applicable probe theory has to be chosen with respect to λ_D, λ_{ei}, and r. By relating these parameters, collisionless or collisional descriptions of particle movement in the plasma sheaths must be applied. For the air plasma the assumption of only single ionized particles and quasineutrality, $n_i = n_e$, is reasonable. The charged particle densities in the investigated regions of the air plasma flow are in the range of $n_e = 10^{17}$ to 10^{21} m^{-3}. With electron temperatures T_e of 5000 to 30,000 K, this results in Debye lengths of $\lambda_D < 40$ μm. The coulomb mean free paths are in the range of $\lambda_{ei} \geq 1$ mm. Therefore, with a typical probe radius of 0.2 mm, the particle movement can be assumed collisionless and can be described by the classical langmuir conventional thin sheath theory, $\lambda_{ei} >> r >> \lambda_D$.

The directed plasma velocities v are up to 5000 m/s close to the exit nozzle of the MPG, expanding against an ambient pressure of 290 Pa. Because most air plasmas are close to full dissociation, the plasma parameters are calculated using the atomic mass of nitrogen. It has been experimentally verified that the collisionless theory of Laframboise for cylindrical probes is valid if the probe is aligned with the plasma flow, and if the probe is long enough and end effects are avoided.[13,14] Within the investigated plasmas, T_e is higher than T_i.

To investigate the energy distribution of the electrons, electrostatic single probes must be used because of their sensitive response to electron currents.[15] Electrostatic single probes, also known as classical langmuir probes, are most commonly used for plasma diagnostics. I is measured as a function of V. For large negative $U = V - V_{PL}$, all electrons are rejected by the probe; only ions are drawn by the probe, resulting in an ion saturation current. For less negative probe voltages in the electron-retarding region of the probe characteristic, an increasing amount of electrons contributes to the net current drawn by the probe, whereas the ion current part decreases. At probe voltages positive with respect to V_{PL}, the ions are rejected and only electrons contribute to the probe current. The shape of the probe characteristic, particularly in the electron-retarding region, where the transition from ion to electron current occurs, is governed by the electron energy distribution function.

For a Maxwellian electron energy distribution function, T_e can be obtained by plotting the slope of the logarithmic electron current in the retarding region vs the probe potential

$$\frac{\mathrm{d}\,\ell n\, I_e}{\mathrm{d}U} = \frac{e}{kT_e} \tag{1}$$

By the theory of Laframboise,[13] j_i to a cylindrical single probe aligned with the plasma is given by

$$I_i = Aen_e\sqrt{(kT_e/2\pi m_i)}\,i_i[\chi_p,\ (T_i/T_e),\ (r/\lambda_D)] \tag{2}$$

The correction factor i_i depends on the normalized probe potential χ_p, the Debye ratio r/λ_D, and the temperature ratio T_i/T_e. The correction factor can be set to 1 in good approximation if the Debye ratio is greater than 50, which can be achieved by choosing the corresponding r in accordance with this requirement,[14] and if the ion current is obtained by the extrapolation of the saturation current region to values of small normalized probe potentials χ_p. V_{PL} can be obtained by the shape of the logarithmic electron current to a single probe.[11] From the measured ion current, which is $I_i = j_i A$, the electron density is calculated for a known probe surface area A.

In the case of deviations from the Maxwellian electron velocity, or rather energy distribution, i.e., one has another isotropic distribution function, this distribution function can be obtained from the probe characteristic in the retarding region at $V < V_{PL}$. The shape of the second derivative of I_e to a single probe with respect to U is proportional to the shape of the distribution function of the electrons, which can be numerically fitted. To do this, V_{PL} must be known, because the probe potential must be calculated with respect to the plasma potential. In the electron-retarding region of the probe characteristic, the change of probe current is mainly driven by the change in the electron current part, which is much greater than the change in the ion current. Thus, it can be assumed that the second derivative of the total probe current is essentially the same as the second derivative of the electron current.

If I_e is differentiated twice with respect to U, one yields

$$F(E)\big|_{E=-eU} = \frac{4}{Ae^2}\sqrt{\frac{-m_eU}{2e}}\,\frac{\mathrm{d}^2I_e}{\mathrm{d}U^2} \tag{3}$$

for the electron energy distribution function of the electrons.[12,15] To handle the obtained probe characteristics for $F(E)$, it is efficient to treat the characteristics numerically using the opportunities offered by modern computer systems, as described in the next section.

The second type of electrostatic probes used to obtain electron temperatures and densities are double probes, which are usually two electrodes of equal areas.[16] The double-probe circuit is an isolated closed floating circuit with both electrodes always negative with respect to the plasma. By applying a voltage difference V between the two electrodes, the more negative electrode draws ion current. Because one of the two electrodes is always more negative, only the ion saturation current region can be reached. Only high-energy electrons penetrate the plasma sheath near V_F and contribute to the net current. T_e is obtained by the equation

$$\left.\frac{\mathrm{d}I}{\mathrm{d}V}\right|_{V=0} = \frac{I_{i1}I_{i2}}{I_{i1} + I_{i2}}\,\frac{e}{kT_e} \tag{4}$$

I_{i1} and I_{i2} are extrapolated from the saturation regions of the characteristic to V_{PL}, where no current is drawn.

The disadvantage of single and double probes is the large heat load during the measurement of the probes in the plasma jet, as a result of the time needed to position the probe and to obtain the probe characteristics in regions close to the plasma generator. The high current to the probe also often results in high thermal loads, leading to extensive erosion in the chemically reacting air plasma. Within such environments, the electrostatic triple probe, which measures the whole radial distribution of the electron temperature and the electron density by a fast radial motion of the probe through the investigated plasma jet, is a commonly used diagnostic tool.[17,18]

The electrostatic triple probe consists of three symmetrical electrodes of A, two of them, 1 and 3, connected as a double probe and a third, 2, floating with respect to the plasma. In a

collisionless thin-sheath plasma, the current to each electrode at a potential V can be expressed by

$$\begin{aligned} -I_1 &= Aj_i(V_1) - Aj_e \exp(-eV_1/kT_e) \\ I_2 &= Aj_i(V_2) - Aj_e \exp(-eV_2/kT_e) \\ I_3 &= Aj_i(V_3) - Aj_e \exp(-eV_3/kT_e) \end{aligned} \tag{5}$$

Without an externally applied potential difference between the double-probe circuit and the floating electrode, the current I_2 to the floating electrode will be zero. Because j_i depends on the electrode potentials, the assumption of equal ion current densities is not quite correct even for the thin-sheath case. Therefore, Chen and Sekiguchi[19] derived an approximate expression for the ion current density that includes a correction factor β. This correction factor scales the potential difference with respect to V_F. Using this correction within the current ratio of the direct display system with the floating single probe, one obtains

$$\frac{1}{2} = \frac{1 - \{(1 - \beta U_2)^{1/2} + [1 + \beta(U_3 - U_2)]^{1/2}\}}{1 - \exp(-eU_3/kT_e)} \times 0.5 \exp\left(\frac{-eU_2}{kT_e}\right) \tag{6}$$

to determine the electron temperature, with $U_2 = V_2 - V_1$, and $U_3 = V_3 - V_1$. For an externally applied fixed potential difference U_3 in the double-probe circuit, an electron temperature-dependent potential voltage difference U_2 can be measured between the double probe and the floating electrode. For high values of U_3, reasonable values of T_e can be directly obtained in a linear dependence on the measured value of U_2. The value for β can be obtained experimentally by the determination of V_F through a single probe characteristic of a triple-probe electrode, or by calculation.[20,21] From the collisionless probe theory and I in the double-probe circuit, the electron number density is determined by

$$n_e = \frac{\sqrt{m_i}I}{A} \frac{1.05 \cdot 10^9 [1 - \beta(V_F - e/2KT_e)]^{1/2}}{\sqrt{T_e}[\exp(eU_2/kT_e) - (1 - \beta U_2)^{1/2}]} \tag{7}$$

For the probe methods of the electron temperature and density measurements described in the preceding text, the uncertainties of local measurements are mainly caused by fluctuations in the high-enthalpy air plasma flow, resulting in mean values with standard deviation error bars larger than those caused by systematic error sources such as misalignment. Because the plasma flow within the high-ambient-pressure vacuum chamber is parallel to the centerline axis, the probe moving through the plasma flow is always aligned with the plasma flow vector, as demanded by the theory of Laframboise.[13] Because of spectroscopic investigations of the air plasma flow, only single ionized species are present, therefore the influence of multiple ionization on the density evaluation can be disregarded.

Time-of-flight probes for velocity measurements are electrostatic double probes separated at a known distance of 25–50 mm and aligned with the flow of the plasma particles. Upstream and downstream probes are both biased to draw ion-saturation current. Fluctuations in the local ion number density around a probe result in fluctuations in the detected ion current. By moving with the flow velocity, those fluctuations are first detected at the upstream probe and then time-delayed at the downstream probe. By performing a fast Fourier transform cross correlation with the two signals, the exact value of the time shift, or rather, the time of flight, can be easily determined. With the known separation of the two probes, the mean velocity of the plasma particles between the two double probes can be calculated.

Theoretically formulated and experimentally verified, the ion current to a cylindrical probe in a plasma flow depends strongly on the angle θ between the probe axis and the plasma flow vector.[22] For a probe electrode not aligned with the plasma flow, the kinetic energy of charged particles moving toward the electrode results in a deformation of the potential sheath around the electrode, in which the charged particles are sampled and contribute to the probe current. For electrodes aligned with the plasma flow vector, only those charged particles that enter the potential sheath by random thermal motion, as with stationary plasmas, contribute to the probe current. In general, the ion current to a probe at an angle θ with respect to the velocity vector can be described by the following equation[22]:

$$I_i = \sqrt{\frac{kT_e}{2\pi m_i}} n_e e A \frac{2}{\sqrt{\pi}} \exp\left[-\left(\frac{v_i}{v_{th}}\right)^2 \sin^2\theta\right] \times \sum_{n=0}^{\infty} \left(\frac{(v_i/v_{th})^{n_{\sin} n_\theta}}{n!}\right)^2 \Gamma\left(n + \frac{3}{2}\right) \tag{8}$$

For two single probes, with one oriented perpendicular, $\sin\theta = 1$, and one aligned with the flow vector, the ratio of the ion currents that can be measured becomes a function of the velocity ratio v_i/v_{th}

$$\frac{I_{i\perp}}{I_{i\parallel}} = \frac{2}{\sqrt{\pi}} \exp\left[-\left(\frac{v_i}{v_{th}}\right)^2\right] \sum_{n=0}^{\infty} \left[\frac{(v_i/v_{th})^n}{n!}\right]^2 \Gamma\left(n + \frac{3}{2}\right) \tag{9}$$

If the ion temperature is known, the thermal velocity can by calculated by

$$v_{th} = \sqrt{2kT_i/m_i} \tag{10}$$

and v_i can be derived from the velocity ratio.[23] Otherwise, the method for ion temperature determination is as follows. By using two crossed single probes, the current ratio and therefore the velocity ratio can be detected. By knowing the directed velocity of the plasma from time-of-flight measurements, T_i can be calculated by Eq. (10).

There are some crucial assumptions underlying the crossed probe method. To obtain the correct current ratio, the surface area of both probes must be known or assumed to be equal. Particularly in chemically reacting air plasmas, a high erosion rate of the perpendicular electrode is observed, which has to be taken into account.[20] Within supersonic flows, such as in MPG plasmas, the effective area of the perpendicular probe changes as a result of wake effects on the backside. A correction factor of 2 for the current to the perpendicular probe can be approximately applied. Because the method of measuring the ion temperature is a combination of two independent methods, the errors are at about $\pm 50\%$ of the absolute value for T_i and at about 20% for v_i.

The dependence of the ion current on θ can also be used for the determination of the plasma flow. If a cylindrical single-probe electrode that rotates in the plasma flow is aligned with the plasma streamlines, $\theta = 0$ deg, the current to the probe must show, according to $\sin\theta = 0$, a minimum if τ_l is greater than 50 for an appropriate electrode length l.[14] Normally, electrodes of $l = 10$ mm are convenient to disregard end effects. In any case, the line shape of the ion current to the single probe vs the angle of attack gives the angle of alignment and, therefore, the plasma flow most common with respect to the plasma jet axis.[24]

Experimental Setup

The electrodes of the cylindrical electrostatic probes are made of tungsten wires typically 0.4 mm in diameter, but the diameter can vary between 0.1 and 1 mm; l is in the range of

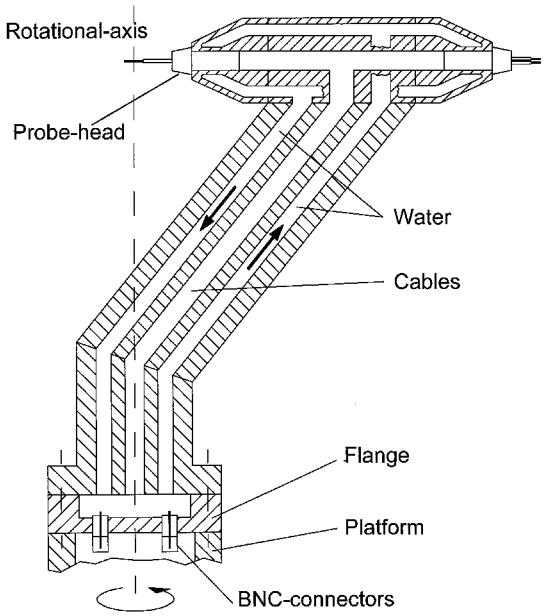

Fig. 2 Probe support.

10 to 20 mm. The electrodes are isolated by alumina tubes of different diameters, depending on the diameters of the electrodes. The electrodes, or rather, the alumina tubes, are mounted in a row in a cylindrical probe head made of brass. The connection to the data acquisition system is performed by heat-resistant and isolated copper wires that are pinched to the electrodes. The construction for single and double probes differs only in the number of electrodes. For crossed single probes, the tungsten wires outside of the isolator are bent to the required angle and direction. The complete probe head can be mounted in one of two possible positions of the probe support (Fig. 2).

Two double probes or a single and a triple probe can be operated by rotating the water-cooled probe support by an angle of 180 deg. The probe support is mounted to the $x-y-z$ platform in the PWK2, which also allows the rotation of the probe support around the z axis. For the determination of plasma streamlines, the probe support was constructed in such a way that the center of a single probe electrode is positioned exactly at the rotational axis.

In the experimental setup of the triple probe, the fixed voltage of the double-probe circuit is applied by an external power supply. The double-probe current is measured as potential drop over a 1-Ω precision shunt of 0.1% accuracy. A transient recorder with a high input impedance of 1 MΩ, which is necessary to measure reliable values of U_2, is used for data acquisition. The same setup is used for single- and double-probe measurements, but the probe potential is then modulated in a sinusodial or sawtooth form with frequencies of up to 1 kHz to acquire current–voltage characteristics. For single probes, the vacuum chamber wall potential is taken as reference potential. The frequency does not have influence on the general shape of the characteristic but should be rather high to avoid smoothing procedures of natural fluctuations, as shown in the Results section. For time-of-flight measurements, the currents to the electrodes are measured by several shunts.

For single-probe data evaluation, as a first step, the Laframboise theory is used to evaluate the electron temperature and the density,[13] based on the assumption of a Maxwell electron energy distribution from the probe characteristic. A first validation of this assumption can be obtained from the linearity of the semilog plot of the electron current.

For a further evaluation of the electron energy distribution function, first the fluctuations of the probe characteristic must be smoothed. This can be done with computers by either calculating the average value over a window of certain data points, which is crucial, particularly in the retarding region of the characteristic, or by fitting an analytical function to the probe characteristic.[15] Once the data are smoothed, a direct numerical second derivation is applied. By using the formula

$$\frac{\delta^2 I_{e0}}{\delta U^2} = \frac{1}{12\Delta U^2}(-I_{e2} + 16I_{e1} - 30I_{e0} \cdots + 16I_{-e1} - I_{-e2}) + \mathcal{O}(\Delta U^4) \tag{11}$$

the local second derivation of the data point I_{e0} can be calculated by including the two data points before, I_{-e2} and I_{-e1}, and after, I_{e2} and I_{e1}, the data point I_{e0} into the calculation.[25] The value ΔU is the constant voltage difference between two data points. The last term on the right-hand side represents higher orders and can be disregarded for the calculation. To compare the second derivation, which is obtained by an experiment with a calculated energy distribution function, either Maxwellian or any other isotropic function, it is necessary to determine the plasma potential to set the origin of the distribution function.

Results

For discussion of the results, the axial distance to the MPG exit plane is notated as the x position, whereas the y position refers to points lying perpendicular to the plasma flow centerline, which is the $y = 0$ mm position. An erosion of the probe's electrodes, and thus a change of the probe's areas A, was taken into consideration, assuming a linear decrease to the final probe dimension after each test.[20] Measurement points are shown with standard deviation error bars. Figure 3 shows two single-probe characteristics on the centerline of the plasma flow at $x = 117$ and 467 mm.

It can be seen that, in the air plasma flow, natural fluctuations in the probe current occur that are necessary for time-of-flight measurements. Without any clear ion saturation region, the shape of the characteristic at $x = 117$ mm differs remarkably from the one at $x = 467$ mm. Both characteristics were smoothed for evaluation. Regarding the two different current axis, the ion saturation current density increases by a factor of about 75.

In Fig. 4, two characteristics at two different y positions at $x = 467$ mm are shown. Both characteristics are of almost similar shape, resulting in only a small decrease in T_e of about 1500 K in the y direction from the centerline to $y = 60$ mm. This temperature difference was also confirmed by the electrostatic double-probe measurements.[15] V_F are at about 2–3 V probe voltage with reference to vacuum chamber wall potential.

The measured profile of the electron temperature and electron density at different cross sections of the plasma flow in the y direction are shown in Figs. 5–8. Figure 5 also includes

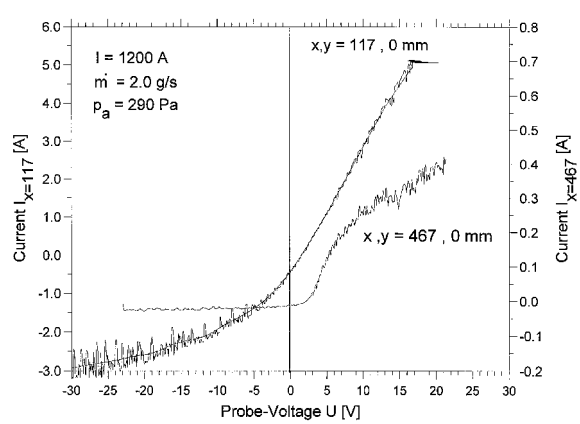

Fig. 3 Single-probe characteristics on the plasma flow centerline at two axial x positions relative to the MPG exit plane.

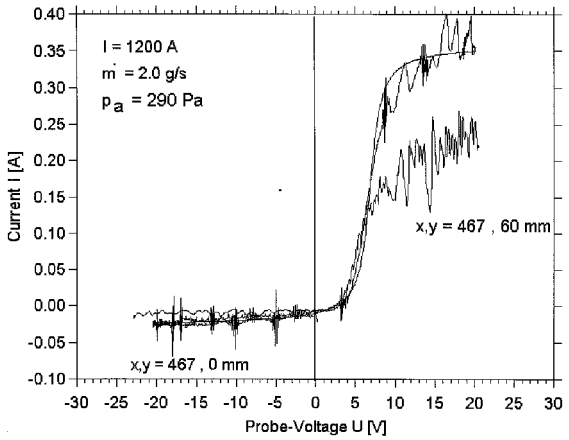

Fig. 4 Single-probe characteristics at two y positions at x = 467 mm to the MPG exit plane.

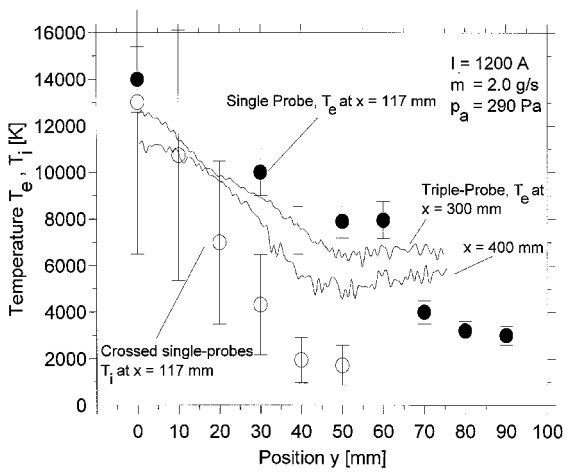

Fig. 5 T_e and T_i distribution at cross sections in different x positions.

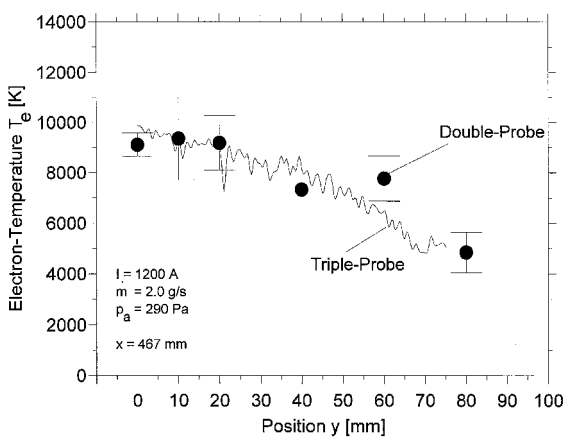

Fig. 6 T_e distribution of the cross section at x = 467 mm.

the ion temperature at x = 117 mm, estimated by crossed single probes and taking into account the velocity measurements shown later. It was difficult to measure profiles in the y direction in the nitrogen–oxygen plasma jet at an axial distance of x = 117 mm, because of the high heat loads and the extreme erosion of the probe electrodes caused by the oxygen. Only one-shot results in the centerline were possible because the probes were destroyed very quickly. As explained later in this paper, the single-probe results close to the plasma source must be seen as the upper limits of the electron temperature because of the deviation of the electron energy distribution from a Maxwellian shape. At x = 467 mm, the results of double and triple probes agree quite well.

In Figs. 9 and 10, T_e and n_e on the centerline are shown as a function of the distance x to the MPG exit plane. Figures 9 and 10 also include the results of emission spectroscopy at positions close to the plasma source, where electrostatic probes cannot be used because of high heat loads. The values of T_e and n_e were obtained by radiative models, taking into account the excitation parameters and visibility of the nitrogen ion lines.[10] The positions of the electrostatic probe measurements correspond to the region of material tests in the plasma wind tunnel. The effect of the Doppler line broadening, measured with Fabry–Perot interferometry, was used to determine T_k of

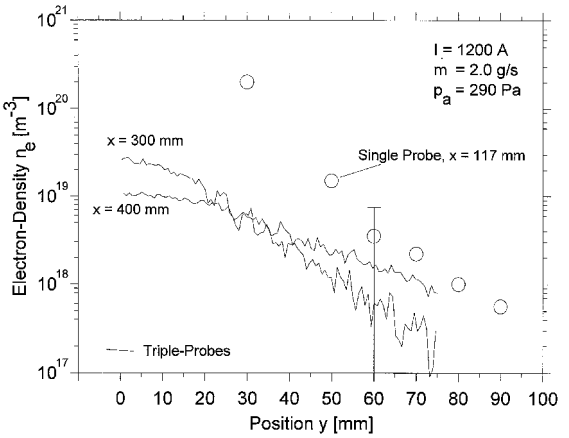

Fig. 7 n_e distribution at cross sections in different x positions.

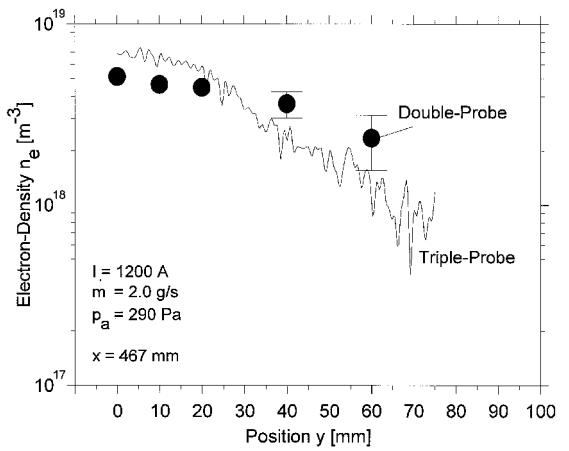

Fig. 8 n_e distribution of the cross section at x = 467 mm.

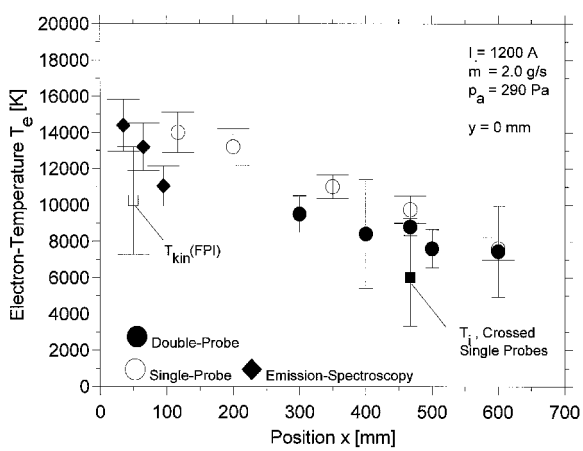

Fig. 9 T_e on the plasma flow centerline, MPG exit at x = 0 mm.

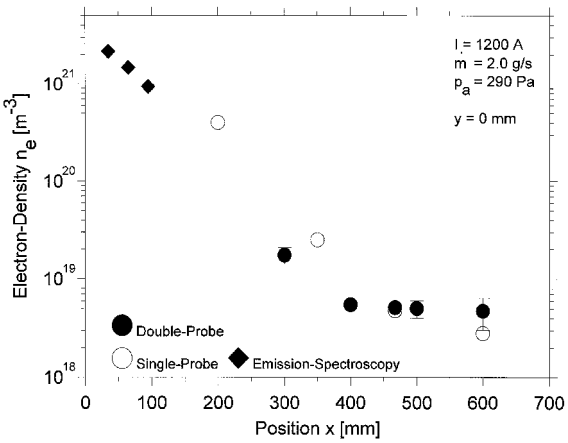

Fig. 10 n_e **on the plasma flow centerline, MPG exit at** x **= 0 mm.**

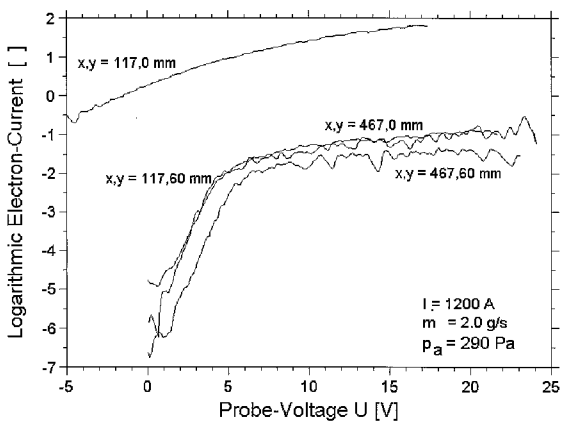

Fig. 11 Semilogarithmic plots of the electron currents to a single probe at different x **and** y **positions to the MPG exit.**

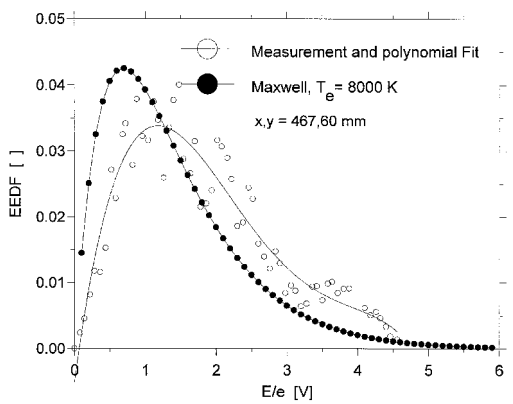

Fig. 12 Experimental and theoretical (Maxwellian) EEDF at x**,** y **= 467, 60 mm.**

the heavy particles, and yielded a value of 10,200 ± 1700 K in the centerline at a distance of x = 50 mm.[14] The difference in the electron density n_e (Fig. 10) from x = 117 to 467 mm, is about a factor of 60. This compares well with the difference of about 75 in the ion saturation current density, a sign for the correct assumption of quasineutrality of the plasma. T_i was estimated, from crossed single-probe and time-of-flight velocity measurements at an axial distance of x = 467 mm, to be about 6000 K.

A first investigation of the Maxwell electron energy distribution is possible by plotting the logarithmic electron current vs the single-probe voltage. For Maxwellian electrons, there should be a linear slope in the retarding region around V_F. V_{PL} is given by the crossing point of the extrapolated linear electron-retarding region and the saturation region of the logarithmic electron current. According to Fig. 11, the electrons on the centerline at x = 117 mm are non-Maxwellian; V_{PL} can be estimated at about 8- to 10-V probe voltage.

In Figs. 12–15, the experimentally obtained electron energy distribution function (EEDF) at different positions in the air plasma are shown. In comparison, Fig. 12 shows also a theoretical Maxwell distribution function related to the measured electron temperature (Fig. 6), of T_e = 8000 K.

For a Maxwell energy distribution function, the amount of higher energy particles increases with the increasing temperature. It can be clearly seen that for the position x, y = 117, 60 mm, which is in the outer region of the plasma flow, and for the positions x, y = 467, 0 mm and x, y = 467, 60 mm, which is far downstream from the MPG exit, the electrons do have a Maxwellian energy distribution. The maximum of the EEDF drops as the electron temperature increases (compare Fig. 12 with Fig. 14). The experimentally obtained EEDF on

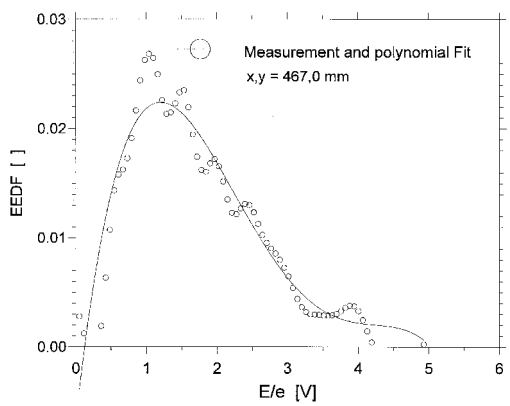

Fig. 13 Experimental EEDF at x**,** y **= 467, 0 mm.**

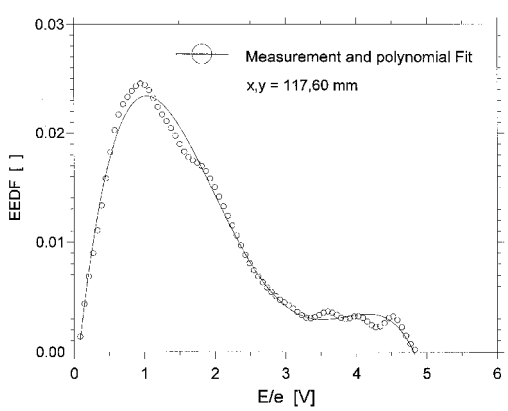

Fig. 14 Experimental EEDF at x**,** y **= 117, 60 mm.**

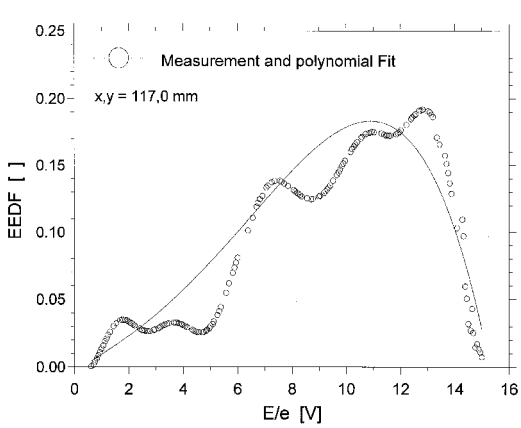

Fig. 15 Experimental EEDF at x**,** y **= 117, 0 mm.**

the plasma flow centerline at x = 117 mm close to the MPG exit is shown in Fig. 15. The EEDF shows large fluctations at this position, and it can be seen that high-energy electrons are dominant. The shape of the distribution function requires further analytical and experimental investigations, e.g., in terms of multiple-electron populations. Also, the transition in the y direction from non-Maxwellian to Maxwellian electrons will be investigated in more detail in future measurements.

A first estimation of the boundaries between Maxwellian and non-Maxwellian electrons in the plasma flow is shown in Fig. 16. Within the light-gray region of this scheme, the distribution function makes a transition from Maxwellian to non-Maxwellian. As an interesting first result, there seems to be a region in the outer part of the plasma flow, at x = 117 mm, where the Maxwellian distribution function penetrates the area of the non-Maxwellian electrons.

Figure 17 shows the axial velocity distribution, which is the velocity component parallel to the plasma flow center axis, at

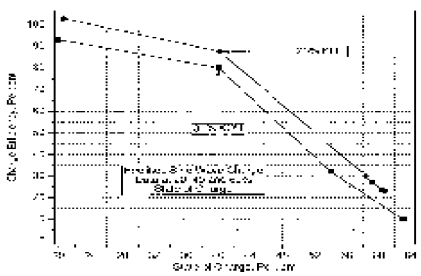

Fig. 16 Estimated regions of Maxwellian and non-Maxwellian electron energies in the air plasma flow. Dots represent data points.

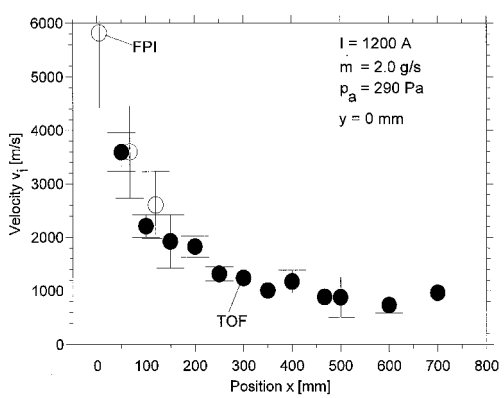

Fig. 17 Axial velocity distribution in the x direction at the plasma flow centerline, measured with time-of-flight probes and Fabry–Perot interferometry.

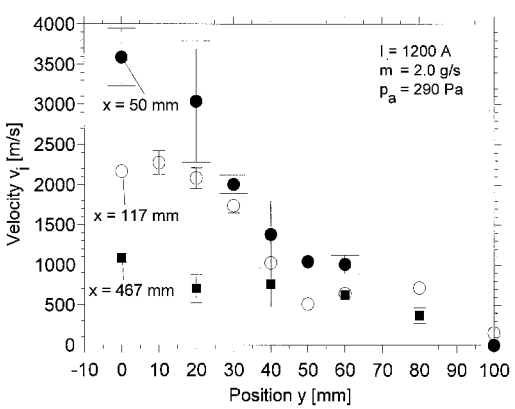

Fig. 18 Axial ion velocities at different y positions, measured with electrostatic time-of-flight probes at different distances of x to the MPG exit.

the centerline of the plasma flow with increasing distance x to the MPG exit. The indicated x positions are corresponding to the center between the two double probes with an accuracy of $\pm$0.5 mm. Axial velocity measurements with time-of-flight probes in the y direction were taken at distances of x = 50, 117, and 467 mm to the MPG. The profiles are shown in Fig. 18.

The centerline velocity at the axial distance of 50 mm is about 3600 m/s, and decreases to about 1000 m/s at x = 467 mm. The velocity measurements, especially those close to the plasma source, were compared with optical velocity measurements using the Doppler-shift effect of a nitrogen-emission line at 746.83 nm, detected with a Fabry–Perot interferometer.[4,20] The measured plasma velocities were also taken as input values for calculation of the stagnation pressures by the Bernoulli equation.[10] The calculated results agreed quite well with experimental measurements of the pressure,[10] thus verifiying the reliability of the velocity measurements.

Conclusions

The electrostatic probes presented were used to investigate in detail the flowing and collisionless air plasma generated by an MPG plasma source. The different probe methods show quite reasonable agreements between the measured values of electron temperatures and densities. The time-of-flight probes are fully qualified, and correspond well to several independent means for application in MPG plasmas. The electrostatic single probe proved to be an efficient method to check for the electron energy distribution function at different positions in a plasma flow. It is possible to obtain the necessary second derivative of the probe current by a solely numerical evaluation of the probe characteristic. The electron temperature in the exit region of the MPG is higher than the heavy-particle temperature, as expected, because of the low-pressure ohmic heating in the arc. As a result of collisional energy transfer, the electron temperature and density decrease downstream. For the investigated air plasma flow, there seems to be a deviation from the Maxwell electron energy distribution function at positions close to the plasma source on the plasma flow centerline. Additional numerical investigations are necessary to characterize the electron relaxation processes in the plasma flow close to the MPG. The results of the electrostatic probe measurements are an important contribution to full characterization of the air plasma flow, experimentally and numerically.

Acknowledgment

This work was supported by the Deutsche Forschungsgemeinschaft within the Sonderforschungsbereich SFB 259-TPA3, Hochtemperaturprobleme rückkehrfähiger Raumtransportsysteme.

References

[1]Auweter-Kurtz, M., Kurtz, H. L., and Laure, S., "Plasma Generators for Re-Entry Simulation," *Journal of Propulsion and Power*, Vol. 12, No. 6, 1996, pp. 1053–1061.

[2]Habiger, H., Auweter-Kurtz, M., and Kurtz, H. L., "Electrostatic Probes for the Investigation of Arc Driven Electric Propulsion Devices," *Proceedings of the 23rd International Electric Propulsion Conference* (Seattle, WA), Vol. 2, 1993, pp. 1137–1147.

[3]Winter, M., Auweter-Kurtz, M., Kurtz, H. L., and Park, C., "Investigation of an Equilibrium Condition Boundary Layer in Front of a Material Probe in a Subsonic Plasma Flow," AIAA Paper 96-1853, June 1996.

[4]Habiger, H., and Auweter-Kurtz, M., "Fabry-Perot Interferometry for the Investigation of a High Enthalpy Plasma Flow," AIAA Paper 95-2040, June 1995.

[5]Auweter–Kurtz, M., Habiger, H., and Wegmann, T., "Diagnostics for High Enthalpy Plasma Flows," AIAA Paper 97-2495, June 1997.

[6]Schönemann, A., and Auweter-Kurtz, M., "Characterization of Nitrogen and Air Plasma Flows by Mass-Spectrometry," 11th International Symposium on Plasma Chemistry, Loughborough, England, UK, March 1993.

[7]Stoeckle, T., Auweter-Kurtz, M., and Laure, S., "Material Catalysis in High Enthalpy Air Flows," AIAA Paper 96-1964, June 1996.
[8]Fasoulas, S., Sleziona, P. C., Auweter-Kurtz, M., Habiger, H., Laure S., and Schönemann A. T., "Characterization of a Nitrogen Flow Within a Plasma Wind Tunnel," *Journal of Thermophysics and Heat Transfer*, Vol. 9, No. 3, 1995, pp. 422–431.
[9]Habiger, H., Auweter-Kurtz, M., Fasoulas, S., Laure, S., and Schönemann, A., "Investigation of a High Enthalpy Air Flow Within a Plasma Wind Tunnel," AIAA Paper 94-2037, June 1994.
[10]Auweter-Kurtz, M., Bauer, G., Behringer, K., Dabalà, P., Habiger, H., Hirsch, K., Jentschke, H., Kurtz, H., Laure, S., Stöckle, T., and Volk, G., "Plasmadiagnostics Within the Plasma Wind Tunnel PWK," *Zeitschrift für Flugwissenschaften und Weltraumforschung*, Vol. 9, No. 3, 1995, pp. 166–179.
[11]Swift, J. D., and Schwar, M. J. R., *Electrical Probes for Plasma Diagnostics*, Iliffe Books Ltd., London, 1970.
[12]Chung, P. M., Talbot, L., and Touryan, K. J., *Electric Probes in Stationary and Flowing Plasmas*, Springer–Verlag, New York, 1975.
[13]Laframboise, J. G., "Theory of Spherical and Cylindrical Langmuir Probes in a Collisionless Maxwellian Plasma at Rest," Univ. of Toronto, Inst. of Aerospace Studies, Rept. 100, Toronto, ON, Canada, 1966.
[14]Hester, S. D., and Sonin, A. A., "Ion Temperature Sensitive End Effect in Cylindrical Langmuir Probe Response at Ionosphere Satellite Conditions," *Physics of Fluids*, Vol. 13, No. 5, 1970, pp. 1265–1274.
[15]Habiger, H., Auweter-Kurtz, M., and Kurtz, H., "Investigation of Electron Energy Distributions in an MPG Arc Jet Flow with Electrostatic Probes," *Proceedings of the 24th International Electric Propulsion Conference* (Moskau), Vol. 1, 1995, pp. 126–133.
[16]Johnson, E. O., and Malter, L., "A Floating Double Probe Method for Measurements in Gas Discharges," *Physical Review*, Vol. 80, No. 1, 1950, pp. 58–69.
[17]Tilley, D. L., Castillo, S., Jolly, M. S., Niewood, E., and Martinez-Sanchez, M., "A Comparison of Theory and Measurements in the Anode Region of a Self-Field Cylindrical MPD Thruster," AIAA Paper 94-3337, June 1994.
[18]Burton, R. L., DelMedico, S. G., and Andrews, J. C., "Application of a Quadruple Probe Technique to MPD Thruster Plume Measurements," *Journal of Propulsion and Power*, Vol. 9, No. 5, 1993, pp. 771–777.
[19]Chen, S. L., and Sekiguchi, T., "Instantaneous Direct-Display System of Plasma Parameters by Means of Triple Probe," *Journal of Applied Physics*, Vol. 36, No. 8, 1965, pp. 2363–2375.
[20]Habiger, H., "Elektrostatische Sonden und Fabry-Perot Interferometrie zur Untersuchung von lichtbogenbeheizten Plasmen für Triebwerks-anwendungen und Wiedereintrittssimulation," Ph.D. Dissertation, Inst. für Raumfahrtsysteme, Univ. of Stuttgart, Stuttgart, Germany, 1994.
[21]Tilley, D. L., Kelly, A. J., and Jahn, R. G., "The Application of the Triple-Probe Method to MPD Thruster Plumes," AIAA Paper 90-2667, July 1990.
[22]Kanal, M., "Theory of Current Collection of Moving Cylindrical Probes," *Journal of Applied Physics*, Vol. 35, No. 6, 1964, pp. 1967–1703.
[23]Poissant, G., and Dudeck, M., "Velocity Profiles in a Rarefied Argon Plasma Stream by Crossed Electrostatic Probes," *Journal of Applied Physics*, Vol. 58, No. 6, 1985, pp. 1772–1779.
[24]Maisenhälder, F., and Mayerhofer, W., "Jet-Diagnostics of a Self-Field Accelerator with Langmuir Probes," *AIAA Journal*, Vol. 12, No. 9, 1974, pp. 1203–1209.
[25]Abramowitz, M., and Stegun, L. E., *Handbook of Mathematical Functions*, 10th ed., Applied Mathematics Series 55, National Bureau of Standards, Washington, DC, 1972.